Effect of Surface Geometric Structure on the Adhesion Force between Silica Particles

Masayoshi Fuji,* Kotoe Machida, Takashi Takei, Tohru Watanabe, and Masatoshi Chikazawa

Department of Applied Chemistry, Graduate School of Engineering, Tokyo Metropolitan University, 1-1 Minami-ohsawa, Hachioji, Tokyo, 192-0397, Japan

Received: April 23, 1998; In Final Form: August 19, 1998

The adhesion force between nonporous and porous silica particles was measured by AFM as a function of relative humidity. Various porous samples were prepared by hydrothermal treatments in different conditions. Geometric structure was evaluated by gas adsorption, and the mechanism of rehydroxylation that occurred in hydrothermal treatments was investigated by silanol density, IR spectra, and immersional heat. The adhesion force was measured by AFM, and the result was compared with the geometric structure and the rehydroxylation process. As a result, we proved that capillary condensation occurred in small spaces between two particles contacting each other after water filled the pores and capillary force appeared to contribute to a steep increase of adhesion force. The adhesion force under low relative pressure was attributed to hydrogen bonding force and reflected both the contact area and hydrophilicity of the surface.

Introduction

Adhesion force has been industrially of great interest in such areas as colloidal dispersion, aggregation, and lubrication. For instance, in the case of the transportation of colloidal raw materials or caking of medical tablets, controlling the adhesion of individual colloid particles has great importance since the adhesion of colloid particles to the wall of machines causes the decrease of the production capacity. In other examples, such as granulation or a spray drying process, the moderate adjustment of adhesion force has been the key technique to avoid the deterioration of the final products.

Because of these industrial problems, many studies have been done to clarify the adhesion force mechanism. Especially in the gas phase, the effect of humidity has been pointed out over the range of 60−80% RH. Fridrun et al.[1] reported the deterioration of pharmaceutical particles over 75% RH, and McFarlane and Tabor[2] found that the adhesion force between spherical beads rose from negligible values below 75% RH to a maximum value at 88% RH. These studies proved that the contribution of capillary force to adhesion force appeared in a highly humid ambience because of the formation of a liquid meniscus between two particles contacting each other. In addition, capillary force is believed to be dominant in adhesion force, and theoretical equations were introduced by Fisher[3] and Israerachvili.[4]

However despite these great interests, relationship between surface geometric structure and adhesion force has not been investigated either sufficiently or quantitatively. Only a few researchers noted briefly that a rough surface provides a reduction of adhesion.[5,6] This was partly because of the limitation in capability of force measurement apparatus. The determination of surface geometric structure and adhesion force measurement could not be studied with respect to the same samples, since the force measurement was applied to only the particles having too small specific surface areas to determine the surface structure precisely.

However, with the advance of the new apparatus, the Atomic Force Microscope (AFM), adhesion force measurement on fine particles which have fairly large surface areas was made possible with much higher sensitivity. Therefore, although originally developed as the surface scanning microscope, AFM has been used as force measurement apparatus from the early 1990s,[7−10] since Ducker et al.[11] first utilized AFM in colloidal force measurement by means of attaching a particle to the top of the scanning probe.

Making use of this new technique, in this work, we investigated the effect of surface geometric structure on adhesion force by using various silica particles with different pore size distribution. For the purpose of controlling the pore size distribution, hydrothermal treatments both in gas and liquid phase were carried out. From the result of adhesion force measurement, we have considered the relationship between the mechanism of water adsorption and the increase of adhesion force. Additionally the influence of the increase of hydrophilicity through hydrothermal treatments was also discussed, especially at low relative humidity.

Experimental Section

Materials. *Reagents.* The nonporous amorphous silica particles (Adma Fine SO-C5; Tatsumori Co., Ltd.) and the porous amorphous silica particles (SYLOSPHERE; Fuji Silysia Chemical Co., Ltd.) were used. The mean diameters of these samples were 1.7 and 3.0 μm, respectively. SO-C5 was synthesized by continuous combustion of silicon particles at 4000 °C, and SYLOSPHERE was produced by sol−gel processing of a metal alkoxide. The Grignard reagent for the measurement of surface silanol (Si−OH) density was synthesized from metal magnesium and methyl iodide.[12]

Surface Treatment. To control the pore size distribution, hydrothermal treatment was carried out on SYLOSPHERE. Sample R-1 was prepared in liquid phase by immersing the SYLOSPHERE in 150 mL of water under ultrasonic wave for 10 min and heated at 80 °C for 3 h. After the thermal process,

* Author to whom correspondence should be addressed at Department of Applied Chemistry, Graduate School of Engineering, Tokyo Metropolitan University, 1-1 Minami-ohsawa, Hachioji, Tokyo, 192-0397, Japan. E-mail: fuji-masayoshi@c.metro-u.ac.jp. Telephone/Fax: +81−426−77−2850.

10.1021/jp981978+ CCC: $15.00
Published on Web 10/07/1998

TABLE 1: Sample Name and the Conditions of Hydrothermal Treatments for SYLOSPHERE[a]

sample name	sample	surface treatment
SO-C5	SO-C5	untreated
SYLOSPHERE	SYLOSPHERE	untreated
R-1	SYLOSPHERE	immersed in 80 °C water for 3 h
R-2	SYLOSPHERE	exposed to water steam in autoclave at 160 °C for 2 h
R-3	SYLOSPHERE	exposed to water steam in autoclave at 180 °C for 2 h

[a] R-1 was obtained in liquid-phase reaction. R-2 and R-3 were prepared in gas-phase reaction.

the obtained R-1 sample was rinsed with acetone to remove the water in the pores and then evacuated for 2 h. The other samples R-2 and R-3 were treated in gas phase by being shielded in an autoclave with nitrogen gas and 100 mL of water, then reacted with water vapor for 2 h at 160 and 180 °C, respectively. These surface treatments were summarized in Table 1.

Surface Characterization. *Gas Adsorption.* Adsorption isotherms of nitrogen at −196 and water at 0 °C were determined by a volumetric method with a homemade multigas adsorption device after outgassing at 200 °C for 4 h under 10^{-5} Torr to ensure that the surface was free from physisorbed water. The usual value of $\sigma_{N_2} = 0.162$ nm^2 was taken as the cross sectional area of a nitrogen molecule, and that of a water molecule was estimated as 0.105 nm^2 considering water molecules are arranged in closest packing over sample surface.[13] The specific surface areas of the samples S_{N_2} were calculated from nitrogen adsorption by the BET method and the pore size distributions were calculated using nitrogen desorption isotherms, following the Dollimore−Heal equation.[14] A value of 0.284 nm is used for the average thickness of a single molecular layer of water.

Silanol Density. It is widely known that not only the change of pore size distribution but also rehydroxylation proceeds with hydrothermal treatment. Therefore the degree of rehydroxylation was evaluated as silanol density. Surface silanol density for the samples was measured by the Grignard method[12] after determining the specific surface area by nitrogen adsorption.

IR Spectra. FTIR measurements were made on an FTIR system 800 (Nicole Co., Ltd.) using a signal gain of 100 scans and a resolution of 2 cm^{-1}. Samples were prepared in the glass cell as a pellet form and outgassed in the same manner as the gas adsorption experiment. The obtained IR spectra was displayed by subtracting the blank spectra of a glass cell.

Heat of Immersion. The degree of rehydroxylation can also be characterized by heat of immersion with water. The measurement of immersional heat was made at 25 °C with a multi micro calorimeter MMC-5111(Tokyo Riko Co., Ltd.). Silica particles were put in a glass ampule, and specific surface area measured was after outgassing in the same manner. The glass ampule was then placed in a calorimeter, until it reached thermal equilibrium at 25 °C. After this preparation, the ampule was broken and the silica powders inside were immersed in water. The liberated heat was recorded, and calibration was done with some blank experiments.

Force Measurements. All the measurements were obtained by AFM SPI300 (Seiko Instruments Co., Inc.) and analyzed using a SPA3700 system. The adhesion force was converted from the force−distance curve[15] in "force curve" mode. In this operating mode, the substrate displacement was controlled by the applied piezovoltage and interaction force was recorded as the voltage from the split photodiode detector. The photodiode

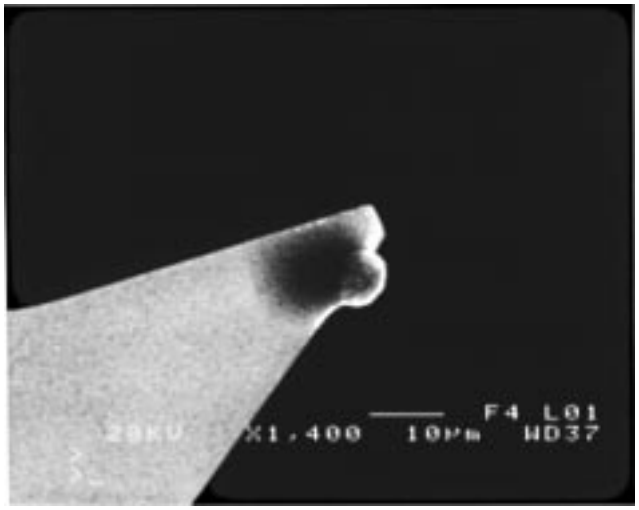

Figure 1. SEM image of a silica particle attached to the top of cantilever.

voltage and piezovoltage were converted via calibration standards to a normalized force−separation distance curve. The frequency was set constant at 3 s, and loading force was kept constant by setting the distance of piezo movement after contact as 200 nm. The value of loading force guarantees enough contact between particles before separation. An optical microscope was used to ensure that the sphere was rigidly on the top of lever. Figure 1 shows a SEM micrograph of a silica particle on the lever.

The other particle in a pair of force measurement was fixed on a flat silicon plate using epoxy resin.[16] Prior to the force measurement, the top of a particle fixed on the substrate was confirmed from a scanning surface image by a cantilever with a sphere, and force was measured between these two particles.

To control the relative humidity, dry nitrogen gas or humid gas was introduced into the AFM head unit at the controlled rate. The value of humidity was recorded by remote controllable measurement. The range of measurement was set from 40% to 90% RH. The lower range of measurement was decided by considering the prevention of extreme electrostatic influences. Nomura et al. reported that the extreme electrostatic influences were found in the range of 15%−40% RH in several powders.[17] The upper limit of humidity measurement was limited by the specification of the humidity sensor. The measurement of adhesional force was performed after waiting sufficient time, which was longer than the adsorption equilibrium time at water adsorption experiments. Therefore, the condition of a water molecule on a silica surface would be regarded as the same as that of adsorption experiment under relative pressure.

The obtained adhesion force f was normalized by the following equation

$$F = f/\left(\frac{1}{R_1} + \frac{1}{R_2}\right) \quad (1)$$

where R_1 is the curvature radius of a silica particle attached to the cantilever and R_2 is that of the particle fixed on the silicon plate. R_1 was calculated through use of an optical microscope, and R_2 was estimated from an AFM cross-sectional image by means of morphological restoration.[18−20]

Results and Discussion

Surface Geometric Structure. Surface specific areas, pore volume, and mean pore radius are listed in Table 2. The specific

TABLE 2: Specific Surface Areas, Pore Volumn and Pore Radius[a]

sample name	specific surface area S_{N_2} ($m^2\ g^{-1}$)	pore volume V_P(mL g^{-1})	pore radius r_m (nm)
SO-C5	3.38		
SYLOSPHERE	532	1.50	4.3
R-1	476	1.40	5.2
R-2	143	1.36	11.7
R-3	74.0	1.36	19.5

[a] Specific surface areas were calculated by the BET method, and pore radius was figured out by using the Dollimore−Heal equation.

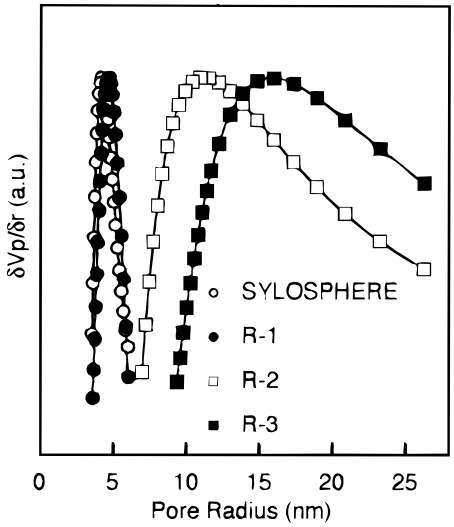

Figure 2. Distribution curves of pore radius calculated from nitrogen desorption isotherms. R-1 showed the curve similar to that of unmodified SYLOSPHERE in contrast to those of R-2 and R-3 which shifted to larger pore radius.

surface areas of untreated porous silica gel SYLOSPHERE are more than 2 orders of magnitude larger than that of nonporous silica SO-C5 owing to numerous pores. However, these large specific areas decreased with hydrothermal treatments, and especially R-2 and R-3 exhibited small areas compared to R-1. On the other hand, the pore volume value was nearly constant throughout all the samples, and pore radius increased with the temperature in inverse proportion to the surface specific areas. Figure 2 shows the pore size distribution for further discussion. Here, one can see that the change of pore size distribution of R-1 is not so significant compared to R-2 and R-3. From the difference, it is assumed that hydrothermal treatments proceed in different extent between R-1 and R-2, R-3. According to Bergna et al.[21] surface dissolution can be divided into two steps. The first step is coalescence which dissolves only silica surface, and the radius of the necks formed among sol particles consisting of primary silica gel is not large enough to result in an extensive loss of specific surface. The second step is a sintering process which is the extensive stage of coalescence, and significant loss of the area caused by widening of the neck radius takes place. In addition, Iler[22] and Leboda and Mendyk[22,23] proposed that the sintering process goes along with the surface fluid of larger pores filling in pores of smaller dimensions and so the pore volume did not change. Therefore, if we assume that SYLOSPHERE should have interstitial pore formed among silica sol particles and the pore radius should be determined by the size of necks among them, we can conclude that R-1 treatment caused only coalescence and R-2 and R-3 treatment proceeded to the extent of the sintering process. The consideration about pore structure was also supported by the shape of the hysteresis loop in the ad−desorption isotherm on SYLOSPHERE for nitrogen.[24] This assumption is schematically show in Scheme 1.

SCHEME 1: Illustration of Surface Sintering Process during Hydrothermal Treatment of R-2 and R-3[a]

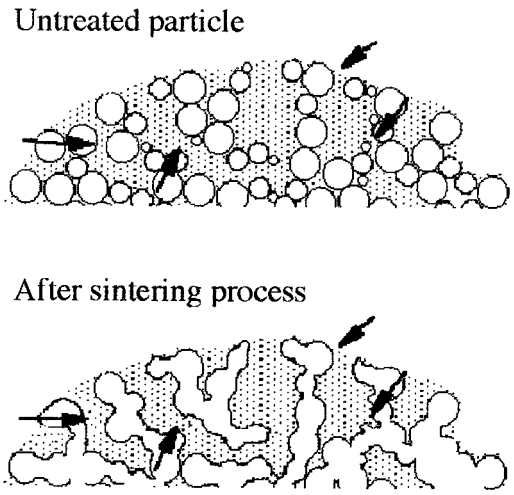

[a] Primary particles consist of small dimensional sol particles (○). The neck of the pore (←) between these sol particles is widened during the sintering process without changing pore volume.

TABLE 3: Silanol Density and Heat of Immersion[a]

sample name	silanol density D_S (OH nm^{-2})	heat of immersion ΔH_{imm}(mJ m^{-2})	heat of immersion per silanol ΔH_{imm} (10^{-21} J OH^{-1})
SO-C5	3.6	190	52.8
SYLOSPHERE	2.6	110	42.3
R-1	3.7	155	41.9
R-2	3.5	180	51.4
R-3	3.6	218	60.6

[a] Heat of immersion was divided by the silanol density to figure out the heat of immersion per silanol.

Rehydroxylation Mechanism. As already mentioned, hydrothermal treatment brings about rehydroxylation as well as surface dissolution. Therefore, we must consider not only the change of surface geometric structure but also the rehydroxylation mechanism.

First, the extent of rehydroxylation can be simply evaluated by the silanol density listed in Table 3. All the treated SYLOSPHERE samples show similar density approximately 3.6 $OH{\cdot}nm^{-2}$, while untreated SYLOSPHERE has only 2.6 $OH{\cdot}nm^{-2}$. Therefore, one can recognize that rehydroxylation occurred in hydrothermal treatments and resulted in the increase of 1.0 $OH{\cdot}nm^{-2}$, independent of any treatments procedures. However, despite the constant value of silanol density, it is induced that the quality of hydroxyl groups is different in each treatment from IR spectra shown in Figure 3. The untreated sample and R-1 displayed similar spectra, and isolated hydroxyl groups peaked sharply at around 3747 cm^{-1}. [22] On the other hand, hydrogen-bonded silanol groups which appeared as broad peaks around 3650 cm^{-1} [22] are more dominant in R-2 and R-3. This means that the rehydroxylation process was different between R-1 and R-2, R-3 and we can assume that this difference contributed to the dissolution mechanism as mentioned above. That is to say, in R-1 treatment, coalescence accompanied only rehydroxylation of strained surface siloxane sites such as two or three-membered rings,[25] whereas the sintering process in R-2 and R-3 drastically changed the surface

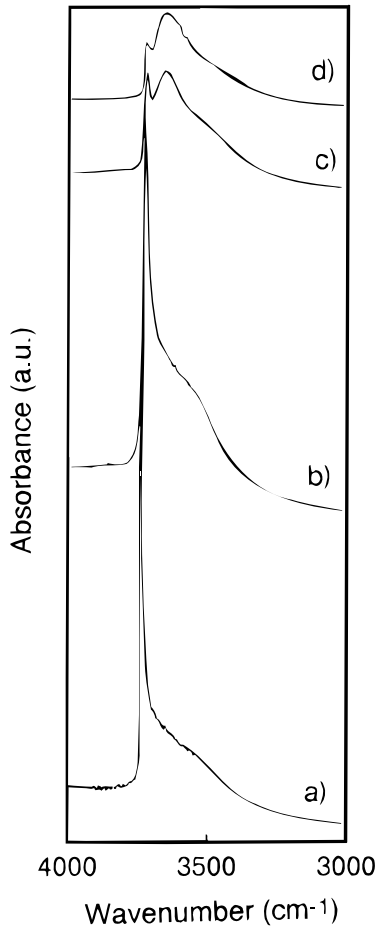

Figure 3. IR spectra from 3000 to 4000 cm^{-1}. The sharp peak at 3747 cm^{-1} and the broad peaks around 3650 cm^{-1} belong to isolated silanols and hydrogen-bonded silanols, respectively. (a) unmodified SYLSOPHERE; (b) R-1; (c) R-2; (d) R-3.

structure by promoting the crystallization and led to the increase of silanol density.[21]

This assumption is supported by the result of immersional heat per silanol listed in Table 3. R-2 and R-3 evolved higher heat of immersion, contrary to R-1 which represented the similar value as untreated sample. Miyata proved that immersional heat per silanol increased with crystallinity[26] and so the increase of immersional heat for R-2 and R-3 indicates that crystallization occurred during the sintering process. This result is quite valid for the assumption of the rehydroxylation mechanism written above.

As a conclusion, we could prove that R-1 treatment proceeded with rehydroxylation, but no significant change of surface geometric structure occurred. On the contrary, R-2 and R-3 treatment brought about rehydroxylation with crystallization and changing the surface geometric structure. The consideration is in good agreement with the conclusion of our previous study[27] concerning change in surface property and structure of porous silica particle by hydrothermal treatment.

Water Adsorption. Both surface chemistry and pore geometry can be clarified also by water adsorption. This is because the shape of the water adsorption isotherm and the amount of adsorbed water are sensitive to surface pore geometry and silanol density. Figure 4 shows the water adsorption isotherms at 0 °C. All the isotherms are categorized as Type III isotherms, and critical increase appeared at high relative pressure. Type III is characteristic of weak gas−solid interaction generally given by a nonporous or mesoporous solid and

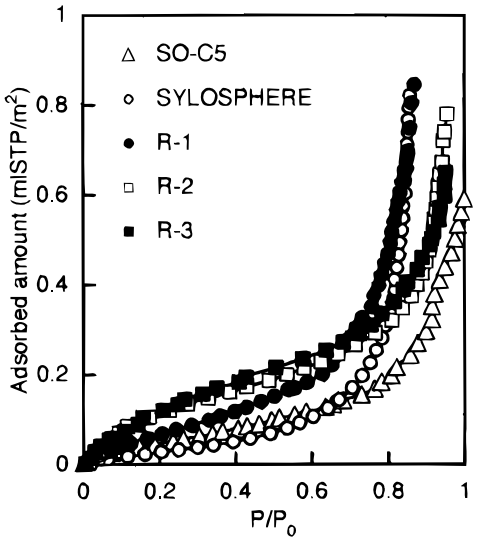

Figure 4. Water adsorption isotherms at 0 °C. All isotherms did not have strong knees at low relative pressure and were categorized in IUPAC III type. This means all the samples do not have micropores.

indicates micropores do not exist on the surface. Consequently, we can recognize that micropores are not involved in SYLOSPHERE samples and the increase of knee at low relative pressure reflects not pore geometry but surface chemistry.[22] Here surface chemistry means the increase of hydrophilicity induced by rehydroxylation or increase of crystallization. The critical increase at high pressure is due to capillary condensation to mesopores or between primary particles. Therefore the critical increase appearing in porous SYLOSPHERE can be assigned to water capillary condensation to mesopores partly including between primary particles, and gradual increase in nonporous SO-C5 is contributed to condensation between primary particles. In addition, the critical pressure was in the order of unmodified $\cong$ R-1 < R-2 < R-3 and coincided with the order of pore radius determined by nitrogen adsorption. This accordance holds true for the Kelvin equation which proved that critical pressure falls with the reduction of pore radius and certified the validity of water adsorptions for these samples.

To conclude, we could confirm the presence of mesopores in SYLOSPHERE, increase of hydrophilicity with hydrothermal treatment, and the critical pressure where capillary condensation occurred.

Adhesion Force Measurements. The main purpose of this study is to elucidate the effect of surface geometry on adhesion force taking the change of hydrophilicity into consideration. We have already clarified the surface geometry and process of rehydroxylation with respect to five samples including nonporous particles as a comparison. On the basis of these experiments, adhesion force between particles was measured as a function of relative humidity.

Figure 5 shows the adhesion force depending on relative humidity approximately in the range of 40−90% RH. Steep increase appeared in SO-C5, SYLOSPHERE, and R-1 unlike in R-2 and R-3 which showed only gradual increase, even at 90% RH. This difference is similar to the difference recognized in geometric structure and the rehydroxylation process. Consequently, we can assume that generation mechanism of the adhesion force is closely related to the surface geometric structure. With respect to nonporous SO-C5, we can easily expect that critical increase of adhesion force appears when capillary force occurs. Actually, the increase from 90% RH is consistent with the increase of water adsorption isotherm which

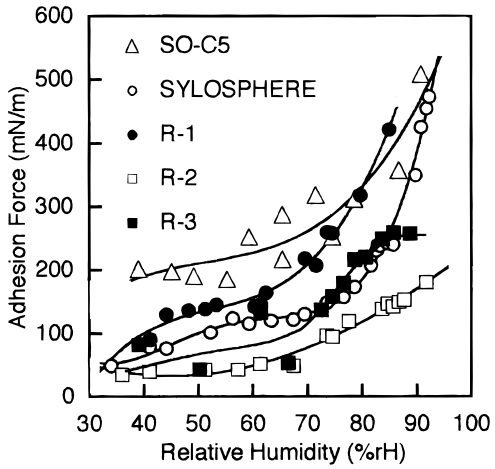

Figure 5. Adhesion force between particles measured by AFM. The obtained data were normalized by eq 1. The critical increase that contributed to the formation of capillary condensation between particles was observed is all except R-2 and R-3.

is due to the capillary condensation between primary particles. However, this explanation cannot be true between rough SYLOSPHERE surfaces. This is because capillary condensation is hindered from forming by the surface asperity, and it was not until extremely high humidity that water filled in the gaps, allowing the capillary force to act in entire area.[28] In the same way, it is estimated that critical increase of adhesion force occurred at the critical humidity where water finished filling the pores and capillary condensation between particles was established. This critical humidity can be calculated by both water adsorption isotherms and the Kelvin equation. The total thickness of the adsorbed water layer t_{ad} and Kelvin radius t_k is equal to the critical pore radius t_r where capillary condensation takes place at each relative pressure p'. The equation was given by

$$t_r = t_{ad} + t_k \tag{2}$$

$$t_k = \frac{V\gamma \cos\theta}{RT \ln p'} \tag{3}$$

where V is molecular volume, γ is surface tension of water, and cos θ represents the water contact angle on the silica surface. The value of t_{ad} was converted from the water adsorbed amount obtained by extrapolating the linear water adsorption isotherm in the region from $P/P_0 = 0.3$ to 0.6. According to eqs 2 and 3 and pore size distribution, we can figure out the critical humidity where water finishes filling all the pores. The result is shown in Figure 6a−d. One can see that critical humidity is about 80% RH for both untreated SYLOSPHERE and R-1; on the contrary, in R-2 and R-3 water still preferentially filled in pores above 95% RH. This result is quite reasonable to explain the steep increase of the adhesion force that appeared in SYLOSPHERE and R-1 over 80% RH and the gradual increase of adhesion force even at 90% RH in R-2 and R-3. Consequently, we could successfully prove the assumption that capillary condensation occurs after water filled the pores quantitatively. (Scheme 2)

On the other hand, to explain the mechanism of adhesion force under low relative humidity, we must consider the effect of hydrophilicity and the contact area between particles since the hydrogen bonding force is dominant instead of capillary force in a low humid ambient.[7] Surface of the porous silica is comprised of solid and pore opening. At low pressure where

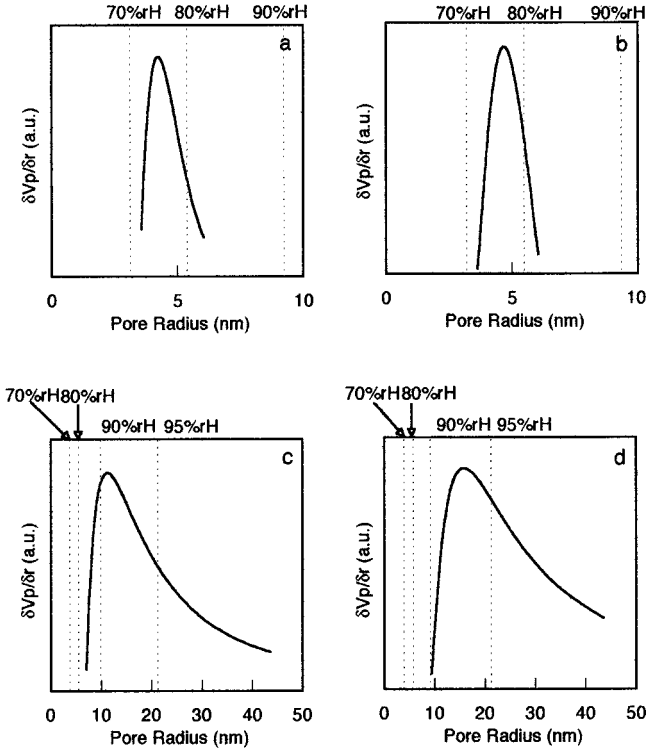

Figure 6. The critical humidity where capillary condensation occurs between particles was calculated by both the Kelvin equation and the thickness of the adsorbed water layer. (a) unmodified SYLOSPHERE; (b) R-1; (c) R-2; (d) R-3.

SCHEME 2: Image of the Formation of Capillary Condensation between Porous Silica Surfaces[a]

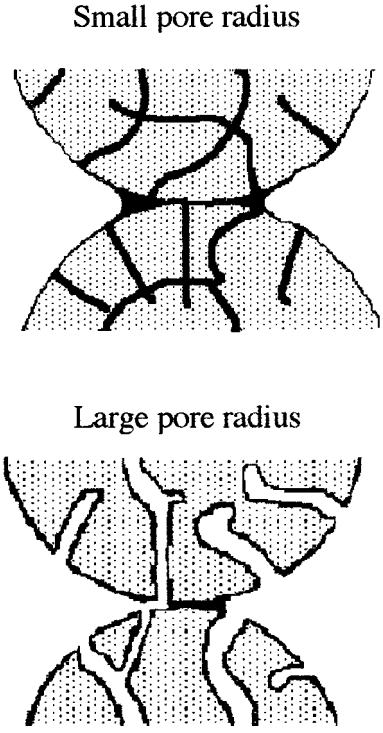

[a] One can see that it is not until water filled in the pores that capillary condensation occurred. Therefore the particles of which pore radius are quite large do not show the critical increase of adhesion force even at 90% RH.

the pores are not yet filled, increase of the adhesion force can only be attributed to the change in the solid part of the surface and physisorbed water on that part. In spite of the fact that the

surface free energy on all samples (including SO-C5) must decrease for adsorbing water molecules, the adhesion force for them tends to increase in Figure 5. These results suggest the formation of a hydrogen bond between particle surfaces using a physisorbed water molecule as intermediate.

Figure 5 shows that the adhesion force of nonporous SO-C5 had larger value than other porous samples. This must be due to the large contact area between the nonporous surfaces. The adhesion force of the porous samples is exhibited as the order R-1 > SYLOSPHERE > R-3 > R-2. We can classify these four samples into two groups from the results of surface geometric analysis. The first group involves SYLOSPHERE and R-1, which have smaller pore radius, and the second group consists of R-2 and R-3, which have larger pore radius. We can see that the larger pore radius decreases the contact area and reduces the adhesion force of the second group. To summarize, it can be determined that the order of adhesion force is SYLOSPHERE, R-1 > R-2, R-3 from the aspect of contact area estimated by the geometric structure. Additionally, rehydroxylation process proved that R-1 has more silanol groups than SYLOSPHERE and crystallization proceeded to a greater extent in R-3 than in R-2. Consequently, in the first group R-1 showed larger adhesion force than SYLOSPHERE, and this was also true for the second group in which R-3 exhibited the larger value compared to R-2.

Conclusions

This study has investigated the effect of geometric structure on adhesion force by controlling the pore radius of silica particles and has clarified the relationship between the establishment of capillary bridge and the increase of adhesion force. In addition, the influence of hydrothermal treatment on adhesion force has been also considered, especially under low relative humidity. We have concluded the following:

(i) The hydrothermal process using boiling water brought about coalescence and rehydroxylation without changing the surface geometric structure significantly. On the other hand, the hydrothermal process using an autoclave caused the sintering of the silica surface with crystallization and led to a widening of the pore radius and reduction of the specific surface area.

(ii) The water adsorption isotherm reflected the geometric structure of silica particles and the increase of hydrophilicity.

(iii) The increase of adhesion force under high relative pressure indicated that capillary condensation occurred after water filled the pores, whereas the adhesion force under low relative pressure was explained to be generated by hydrogen bonding force and so depends on the contact area and hydrophilicity.

Acknowledgment. The author is grateful to Tatsumori Co., Ltd. and Fuji Silysia Chemical Co., Ltd. for providing Adma Fine SO-C5 and SYLOSPHERE, respectively.

References and Notes

(1) Fridrun, P.; Newton, J. M.; James, M. B. *Int. J. Pharm.* **1996**, *145*, 221.

(2) McFarlane, J. S.; Tabor, D. *Proc. R. Soc. London* **1950**, *A 202*, 224.

(3) Fisher, R. A. *J. Agric. Sci*. **1926**, *16*, 492.

(4) Fisher, L. R.; Israerachvili, J. *J. Colloid Interface Sci.* **1981**, *80*, 528.

(5) Houston, M. R.; Howe, R.T.; Maboudian, R. *J. Appl. Phys.* **1997**, *81*, 3474.

(6) Yamaguchi, T.; Tomita, M.; Chikazawa, M.; Kanazawa, T. *J. Soc. Powder Technol.* **1979**, *16*, 517.

(7) Veeramasuneni, S.; Yalamanchili, M. R.; Miller, J. D. *J. Colloid Interface Sci.* **1996**, *184*, 594.

(8) Toikka, G.; Hayes, R. A.; Ralston, J. *J. Colloid Interface Sci.* **1996**, *180*, 329.

(9) Biggs, S. *Langmuir* **1995**, *11*, 156.

(10) Larson, I.; Drummond, C. J.; Chan, D. Y. C.; Grieser, F. *J. Am. Chem. Soc*. **1993**, *115*, 11885.

(11) Ducker, W. A.; Senden, T. J.; Pashley, R. M. *Nature* **1991**, *353-(19)*, 239.

(12) Fripiat, J. J.; Uytterhoeven. J. *J. Phys. Chem.* **1962**, *66*, 800.

(13) Fuji, M.; Iwata, H.; Takei, T.; Watanabe, T.; Chikazawa, M. *Adv. Powder Technol.* **1997**. *8*. 210.

(14) Dollimore, D.; Heal, G. R. *J. Appl. Chem.* **1964**, *14*, 109.

(15) Mizes, H. A.; Loh, K. G.; Miller, R. J. D.; Ahuja, S. K.; Grabowski, E. F. *Appl. Phys. Lett*. **1991**, *59* (22), 2901.

(16) Shakesheff, K. M.; Davis, M. C.; Jackson, D. E.; Roberts, C. J.; Tendler, S. J. B.; Brown, V. A.; Watson, R. C.; Barrett, D. A.; Shaw, P. N. *Surf. Sci. Lett*. **1994**, *304*, 393.

(17) Nomura, T.; Yamada, Y.; Masuda, H. *Kagaku Kogaku Ronbunshu* **1998**, *24*, 585.

(18) Mulvaney, P.; Ciersig, M. *J. Chem. Soc., Farady Trans.* **1996**, *92* (17), 3137.

(19) Kardassi, D.; Tsiourvas, D.; Paleos, C. M. *J. Colloid Interface Sci.* **1997**, *186*, 203.

(20) Junno, T.; Anad, S.; Deppert, K.; Montelius, L.; Samuelson, L. *Appl. Phys. Lett.* **1995**, *66* (24), 3295.

(21) Bergna, H. E. *The Colloid Chemistry of Silica*, 1st ed.; American Chemical Society: Washington, DC, 1994.

(22) Iler, R. K. *The Chemistry of Silica*; Wiley-Interscience Publication: New York, 1979.

(23) Leboda, R.; Mendyk, E. *Mater. Chem. Phys.* **1991**, *27*, 189.

(24) Gregg, S. J.; Sing, K. S. *Adsorption, Surface Area and Porosity*; 2nd ed.; Academic Press: London, 1982.

(25) Silva, A. D.; Donoso, P.; Aegerter, M. A. *J. Non-Cryst. Solids* **1992**, *145*, 168.

(26) Miyata, K. *Hyoumen* **1967**,*7* (5), 279.

(27) Fuji, M.; Machida, K.; Takei, T.; Watanabe, T.; Chikazawa, M. *J. Soc. Powder Technol., Japan* **1998**, *35*, 706.

(28) Israelachivili, J. N. *Intermolecular and Surface Forces*, 2nd ed.; Academic Press: New York, 1991.